J. Plasma Fusion Res. SERIES, Vol.1 (1998) 118–121

# High Power EC and NB Heating Experiments in CHS

KUBO Shin*, OSAKABE Masaki, IDEI Hiroshi, KANEKO Osamu, TSUMORI Katsuyoshi, YOSHIMURA Yasuo, IDA Katsumi, NISHIMURA Shin[1], TANAKA Kenji, OKAMURA Shoichi, SHIMIZU Akihiro[2], MINAMI Takashi, ISOBE Mitsutaka, KONDO Takashi[1], SASAO Mamiko, DARROW, Douglass S.[3], MORITA Shigeru, TAKECHI Manabu[2], TAKAGI Shoji[2], OHDACHI Satoshi, TOI Kazuo, TAKAHASHI Chihiro, AKIYAMA Ryuichi, INOUE Noriyuki, SAKAMOTO Ryuichi, WATARI Tetsuo and MATSUOKA Keisuke

*National Institute for Fusion Science, Oroshi-cho, Toki, 509-5292 Japan*

[1]*Graduate University for Advanced Studies, Hayama 240-0193, Japan*

[2] *Dep. of Energy Eng. Science, Nagoya Univ., Nagoya 464-8603, Japan*

[3]*Princeton Plasma Physics Laboratory, Princeton, NJ 08543, USA*

(Received: 30 September 1997/Accepted: 12 January 1998)

**Abstract**

High power heating experiments combining electron cyclotron heating (ECH) and neutral injection beam (NBI) are performed with two gyrotrons and two neutral beam injectors. The classical effect to increase the effective energy input from neutral beam to ions and from electron to ions by increasing the electron temperature is expected. In addition to this classical effect, the change in the potential structure which can be stimulated by adding ECH is expected to change the high energy and/or bulk ion confinement. The results from this high power heating experiment are reported.

**Keywords:**

electron cyclotron heating, neutral beam injection, helical confinement, plasma heating, high $T_i$ mode, CHS

## 1. Introduction

High power heating experiment using two neutral beams and two gyrotron systems are performed in CHS. The aim of this campaign is to get high performance plasma using the maximum heating power available. For the neutral beam injection, the higher the electron temperature, the higher ion heating efficiency is expected from the classical NB heating mechanism[1,2]. The superposition of the ECH and raising electron temperature by factor of 2 are tried. In the previous experiment, however, the drop of the electron density and the transition of the electric potential to positive are observed[3]. The high ion temperature mode in the low density NBI plasma is characterized by the peaked electron density profile and high ion temperature which are observed both in Heliotron-E and CHS[4,5]. The effect of the ECH on this high $T_i$ mode is also observed in Heliotron-E[5] where, the superposition of the ECH degraded the high $T_i$ mode despite of the increase in electron temperature. The effect of the potential is important. The change in the electric field might cause the change in the high energy ion confinement. In the case of the ECH superposition, the enhanced loss of high energy ions are observed[6]. Formation of the electric potential might explain these phenomena. Another example of the effect of ECH on NBI plasma is the observation of the pulsation[7],

**Corresponding author's e-mail: kubo@lhd.nifs.ac.jp*

which is also discussed in relation to the change in the electric potential. The results of high power heating experiments are reported, where the effects of on- and off-axis ECH are investigated.

## 2. Experiments

### 2.1 Heating systems

Neutral beam system installed on CHS has two beam lines, NBI#1 and NBI#2. The injection angle of NBI#1 can be changed from nearly perpendicular to parallel. In the experiment reported here, the beams are injected to the co- and counter directions to reduce the effect of beam driven current. The energy and power of each beam are 40 keV, 1 MW and 35 keV, 800 kW, respectively. ECH system consists of three gyrotrons and two quasi-optical transmission and injection systems. Two of the gyrotrons are used in the experiment described in this report. One of the gyrotron oscillates at 53.2 GHz with the power of 400 kW and the other at 106.1 GHz with 450 kW. The output power is transmitted and injected in CHS via quasi-optical mirror transmission and injector system[8], for fundamental and second harmonic heating at nominal magnetic field of 1.76 Tesla, where, the EC fundamental and second harmonic resonance layers pass the magnetic axis in the case of magnetic axis $R_{ax}$ is set at 0.921 m. The focal point of each injector can be controlled independently.

### 2.2 High Power Heating Experiments

The temporal evolution of the typical plasma parameters is shown in Fig. 1. The initial target plasma for NBI is produced by both fundamental and second harmonic ECH with 10 ms pulse. The line averaged electron density reaches $0.5 \times 10^{19}$ m$^{-3}$. After the injection of the co-NBI#1, electron density gradually increases up to $1.0 \times 10^{19}$ m$^{-3}$, where the largest ion temperature increase is observed by adding the counter NBI#2. Three cases of without, with on-axis and with off-axis second harmonic ECH are compared to see the effect of ECH. The on- and off-axis ECH is achieved by changing the beam focal point of second harmonic ECH while that of fundamental ECH is kept on axis. The off-axis described in this report is the case when the beam focal point is on about 1/3 of the minor radius, and the expected width of the power deposition region from ray tracing calculation is about 1/10 of the minor radius for both on- and off-axis cases.

The electron temperature profile before the injection of NBI#2 is shown in Fig. 2(a). The electron temperature at the center $T_{e0}$ is about 0.6 keV in the case of no ECH. $T_{e0}$ reaches to 1.5 keV and the profile

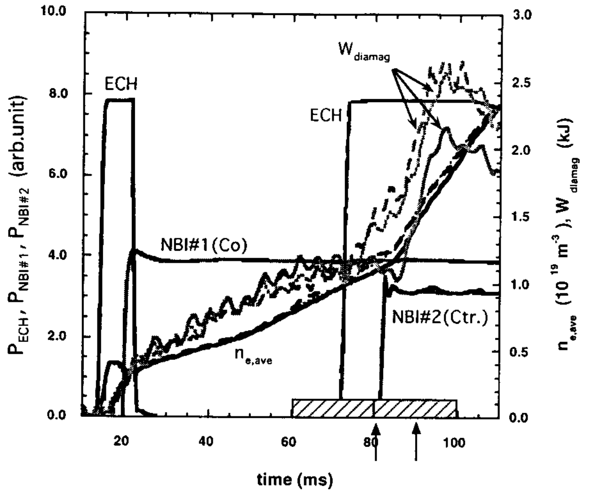


Fig. 1 Time evolution of the heating power, line averaged electron density, stored energy. Thick and broken and dotted line indicates the cases for without ECH, with on-axis ECH, and with off-axis ECH, respectively. The timings of the electron temperature and density profile and ion temperature profiles are shown with arrows and hatched region.

becomes peaked in the case of on-axis ECH and to 1.2 keV and profile becomes broad in the off-axis case. These indicate that power deposition to the electrons is well controlled by ECH. The electron density profiles are shown in Fig. 2(b). The electron density profile shows relatively peaked profile and manifests a specific feature of the high $T_i$ mode[4]. The density profile barely changes by on- or off-axis ECH. Accordingly, the ion temperature profiles show the similar profile and central values observed in high $T_i$ mode[4] but without any significant change due to ECH as shown in Fig. 2(c). Here, the ion temperature profile is measured by charge exchange recombination spectroscopy during 60 to 80 ms in Fig. 1. The central ion temperature is about 0.7 keV.

After the injection of NBI#2, the electron density abruptly increases probably due to the enhanced recycling or increase in impurity influx by the direct loss of high energy ions to the inner wall. This increase in the density due to counter NBI could not be reduced during this experimental campaign despite of several wall conditionings. The temporal evolution of the ion temperature $T_{i,NPA}$ measured by the neutral particle analyzer shows the increase in $T_{i,NPA}$ due to NBI#2 up to the time when the averaged density reaches $1.5 \times 10^{19}$ m$^{-3}$. Abrupt decrease in $T_{i,NPA}$ is seen over this density. These characteristics are not affected by on- or off-axis ECH. The electron temperature profiles at the time of

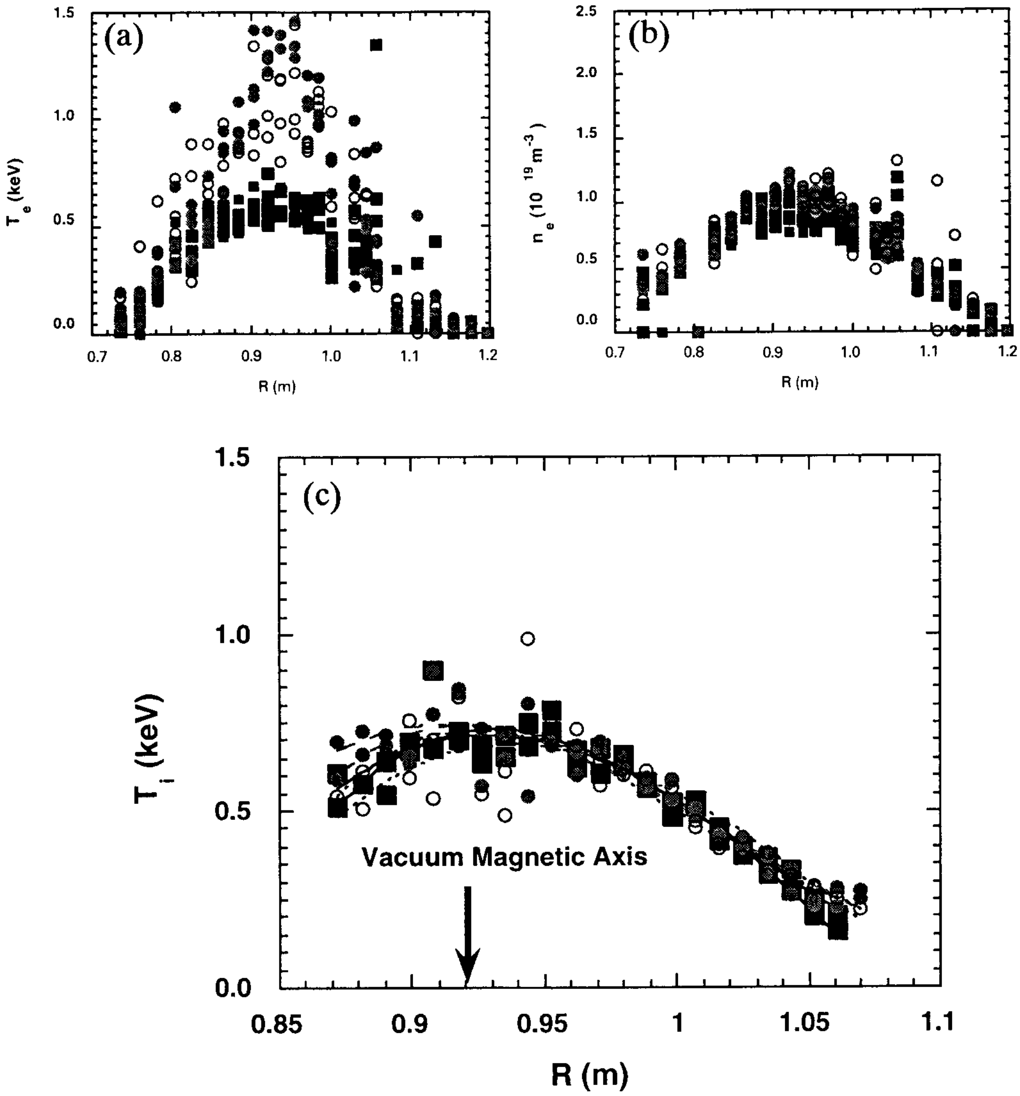


Fig. 2 The profiles of (a) electron temperature, (b) electron density and (c) ion temperature with only NBI#1 injection. The closed square, closed and open circles show the cases without ECH, with on-axis ECH and with off-axis ECH, respectively.

highest $T_{i,NPA}$ are shown in Fig. 3(a). $T_{e0}$ shows a little increase as compared with the case without NBI#2 even though the electron density becomes 1.5 times, which indicates the existence of the substantial power flow from NBI#2 to electrons. In the case of ECH superposition, $T_{e0}$ is kept more than 1 keV for on-axis ECH and just below 1 keV for off-axis ECH. The electron density profiles again show relatively peaked profile and almost no significant change due to on- and off-axis ECH. In Fig. 3(c) are shown the ion temperature profiles when the NBI#2 is superposed. The ion temperature reaches more than 0.8 keV for no ECH case. When the ECH is superposed, $T_i$ tends to be a little lower but is kept at the similar level within the accuracy of the measurement.

## 3. Summary and Discussion

The highest central ion temperature 0.8 keV is achieved in CHS at the density of $1.5 \times 10^{19}$ $m^{-3}$ by superposing two neutral beams. The electron temperature was raised from 0.6 to 1.2 keV by adding ECH on this high ion temperature plasma. The effect of ECH observed so far on this high ion temperature plasma is only raising the electron temperature. The additional effects, which are the change in ion energy flow or confinement by the variation of target electron temperature

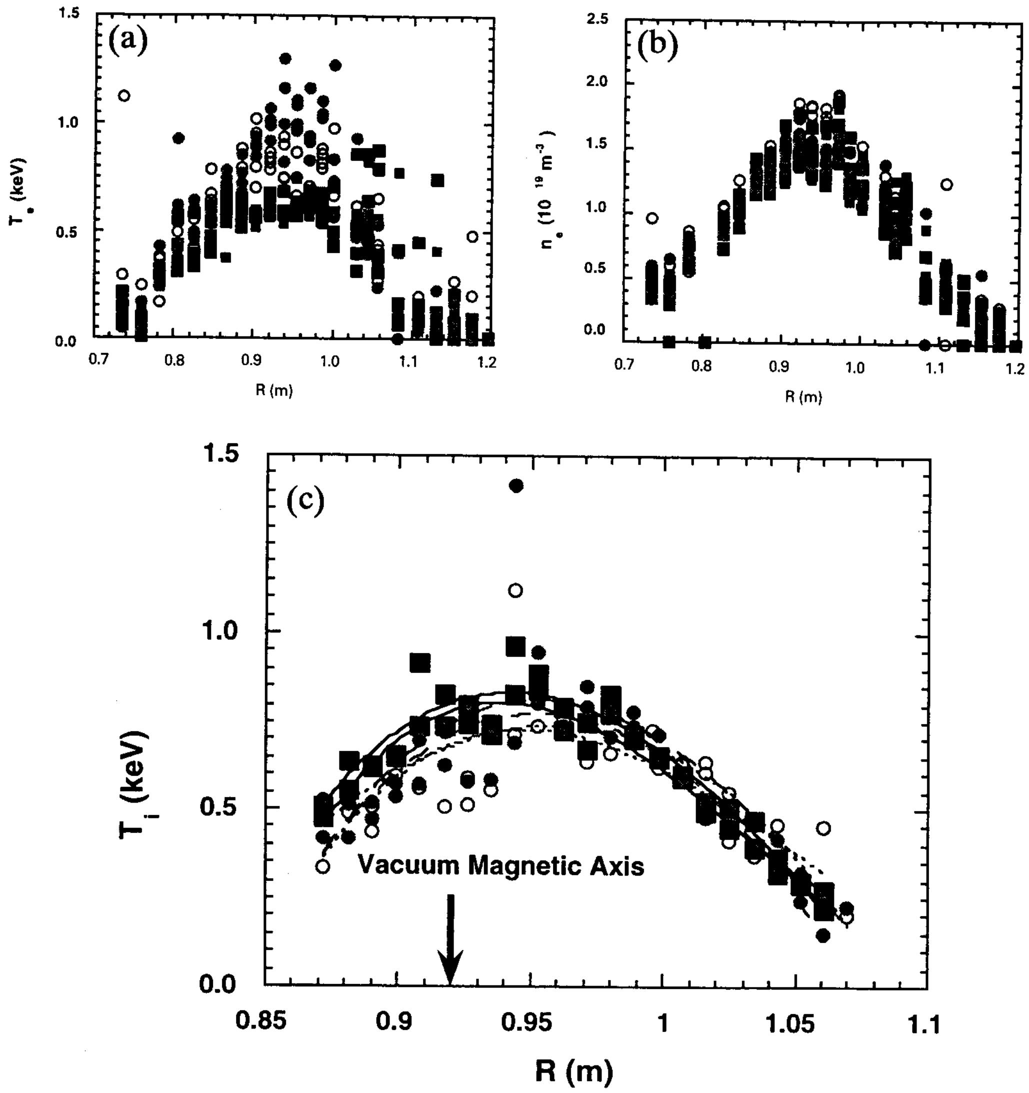


Fig. 3 The profiles of (a) electron temperature, (b) electron density and (c) ion temperature with NBI#1 and NBI#2. The closed square, closed and open circles show the cases without ECH, with on-axis ECH and with off-axis ECH, respectively.

and/or electric potential profile, have not been observed clearly so far. The parameter range during this campaign stays in the plateau regime in the electron collisionality. The further effort to reduce the increase in electron density due to the counter NBI injection is necessary not only to attain the high ion temperature but also to achieve low collisionality regime and to see clear effect of ECH.

## References


[1] T.H. Stix, Plasma Phys **14**, 367 (1972).

[2] M. Osakabe *et al.*, in these Proceedings, p.318 (1998).

[3] H. Idei *et al.*, Phys. Rev. Lett. **71**, 2220 (1993).

[4] K. Ida *et al.*, in these Proceedings, p.239 (1998); T. Minami *et al.*, in these Proceedings, p.243 (1998); K. Tanaka *et al.*, in these Proceedings, p.247 (1998).

[5] K. Ida *et al.*, 16th IAEA Fusion Energy Conference, Montréal, Canada, 1996, IAEA-CN-64/CP-5.

[6] D.S. Darrow *et al.*, in these Proceedings, p.362 (1998).

[7] A. Fujisawa *et al.*, Phys. Rev. Lett. **79**, 1054 (1997).

[8] S. Kubo *et al.*, Fusion Engineering and Design **26**, 319 (1995).